

Chapter 2

Experimental Apparatus

2.1 The Large Hadron Collider

2.1.1 Design

The Large Hadron Collider (LHC) [1] was constructed between 1998–2008 at CERN, the European Centre for Nuclear Research. It occupies the same 27 km circumference tunnel, 100 m below ground, that originally housed the Large Electron-Positron (LEP) [2–4] collider. It accelerates counter-rotating beams of protons to speeds much greater than $0.999c$ before bringing them to collision at one of four main interaction points (IPs) positioned around the ring. The LHC is the largest, highest energy and highest luminosity particle accelerator ever constructed.

There are four main experiments operating at the LHC. ATLAS (cf Sect. 2.2) and CMS [5] (Compact Muon Solenoid) are general-purpose detectors designed with a broad physics programme in mind. From performing precision measurements that test and constrain the Standard Model, to discovering the long-sought Higgs boson and searching for new physics such as Supersymmetry and new heavy particles, these detectors are able to observe a wide range of particles and physical phenomena. The LHCb [6] (LHC beauty) experiment is a single arm forward spectrometer whose main goal is to study heavy flavour physics and the parameters of CP-violation. These studies aim to help explain the matter-antimatter asymmetry in the universe. ALICE [7] (A Large Ion Collider Experiment) is focussed mainly on the study of heavy-ion (lead-lead and proton-lead) collisions. The quark-gluon plasma produced in the extremely high density conditions is of great interest. The main experiments are situated in four of the eight octants that make up the LHC. ATLAS and CMS are located in newly excavated caverns at IP 1 and IP 5. LHCb and ALICE can be found in caverns at IP 2 and IP 8 respectively.

Before entering the LHC itself, beams of protons pass through a series of accelerators in the CERN complex (cf. Fig. 2.1) Once the protons have been accelerated to an energy of 450 GeV they are injected into the LHC ring, and over the course of around 20 minutes are accelerated further until they reach an energy sufficient for

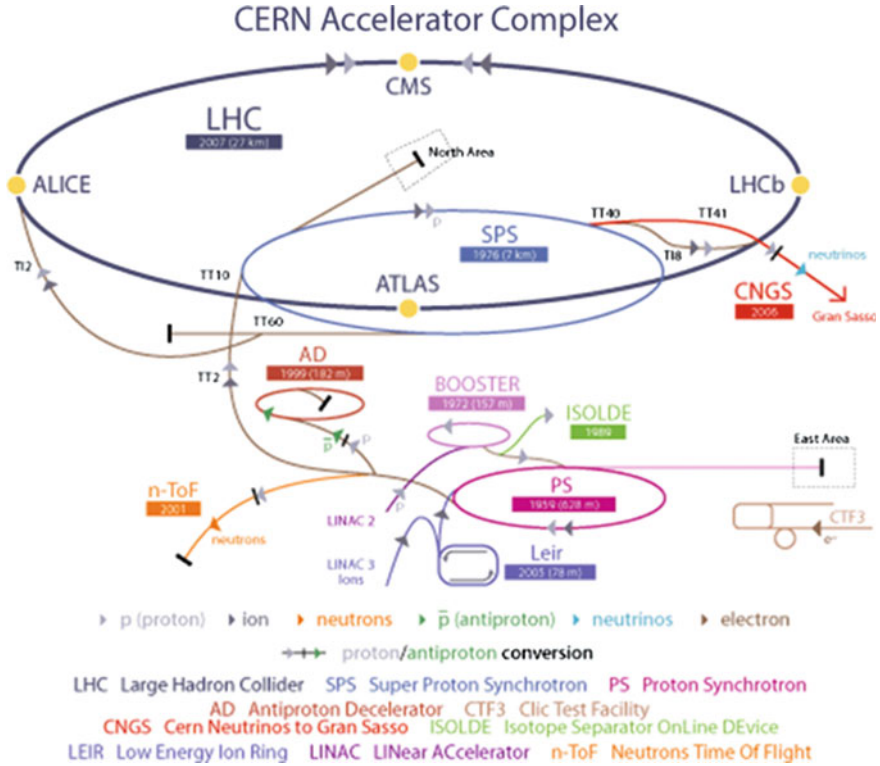


Fig. 2.1 A schematic layout of the accelerator complex and some of the detectors operating at CERN

collisions. The LHC is designed to be capable of colliding proton beams each with energies of 7 GeV.

Protons in each beam are arranged in bunches. One bunch consists of around 1×10^{11} protons, with each LHC ring capable of holding 2808 bunches. The bunches travel in trains, with bunch trains being brought to collision with a design frequency of 40 MHz. The luminosity, \mathcal{L} , of a pp collider can be expressed as [8]

$$\mathcal{L} = \frac{n_b f_r n_1 n_2}{\pi \Sigma_x \Sigma_y}, \quad (2.1)$$

where n_b is the number of colliding bunches, f_r is the LHC revolution frequency (11245.5 Hz), n_1 and n_2 are the number of protons per bunch in colliding beams 1 and 2, and Σ_x and Σ_y characterise the horizontal and vertical beam widths.

2.1.2 Performance

The LHC was designed to operate with a centre-of-mass energy of 14 TeV. However after a very brief nine-day commissioning period in 2008 a faulty electrical connection led to a ruptured liquid helium tank and caused around 6 tonnes of liquid helium to escape into the vacuum pipe. This caused damage to over fifty of the LHC's superconducting magnets and delaying the start of the detectors' data-taking programme by fourteen months.

After the repairs, a short run of collisions with centre-of-mass energy 900 GeV began in November 2009. Following this, high-energy data-taking started again on 30th March 2010 at a centre-of-mass energy of 7 TeV. The LHC continued operating with 3.5 TeV beams throughout 2011 and by the end of its initial data-taking period the LHC had delivered 5.61 fb^{-1} of data, which ATLAS collected with $\approx 94\%$ efficiency. A brief shutdown took place at the start of 2012, before collisions were started again with a centre-of-mass energy of 8 TeV. Throughout 2012 the LHC again exceeded expectations and delivered 23.3 fb^{-1} by the end of the year. Starting in February 2013 the LHC was shut down for repairs and upgrades to be made to the machine. Proton-proton collisions will take place again in early 2015, with beam energies close to the design energy of around 7 TeV (Fig. 2.2).

The bunch spacing was decreased steadily during 2011 to a peak value of 50 ns, corresponding to a maximum of colliding 1380 bunches within the machine at one time. Peak instantaneous luminosity was reached in 2012 at a value of around $7 \times 10^{33} \text{ cm}^{-2} \text{ s}^{-1}$. Such a high instantaneous luminosity led to great challenges in dealing with pile-up. In-time pile-up refers to multiple proton-proton collisions taking place within one bunch crossing, and can be quantified by considering the average number of interactions per bunch crossing, $\langle \mu \rangle$. The peak values for the 7 and 8 TeV data-taking periods were 9.1 and 20.0 respectively, as shown in Fig. 2.3. Out-of-time

Fig. 2.2 Cumulative luminosity versus time delivered to (green), and recorded by (yellow) ATLAS during stable beams and for pp collisions at 7 and 8 TeV centre-of-mass energy in 2011 and 2012 [9]

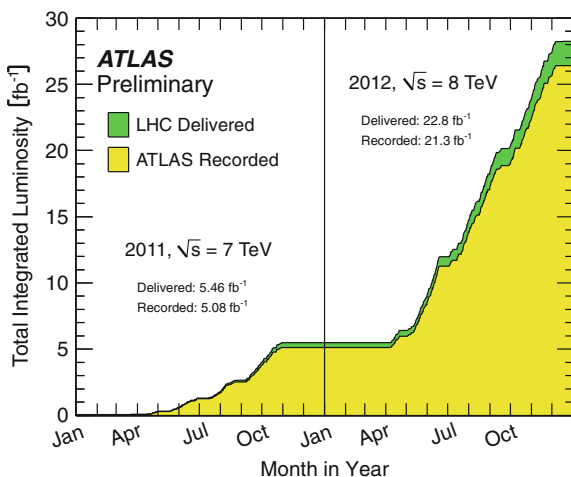
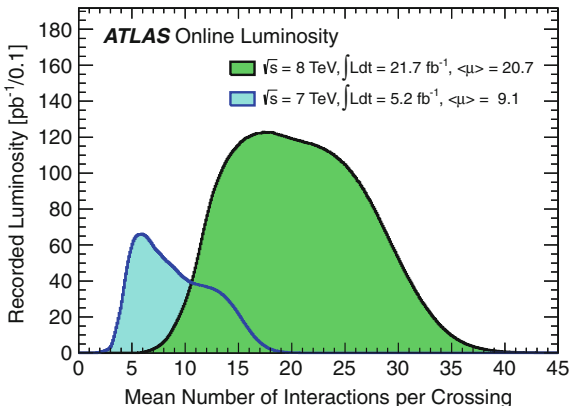


Fig. 2.3 The average number of interactions per bunch crossing during the 7 and 8 TeV data-taking periods [10]



pile-up occurs due to the read-out time of the detector, when particles produced in successive bunch crossings overlap and are read out as part of the same event. Pile-up affects much of the physics being performed at the LHC, from reconstructing vertices and tracks to measuring the energy of hadronic jets. Understanding and limiting the effects of pile-up on the reconstruction of physics objects has been, and will continue to be, crucial to the success of physics analyses.

2.2 The ATLAS Detector

The ATLAS detector was constructed by institutes in 34 countries, and assembled in the cavern at IP 1 around the LHC ring between 2003 and 2008. With a volume of over 1000 m³ and weighing in at around 7000 tonnes it is the largest of the four main detectors.

The coordinate system employed by ATLAS is right-handed, with the z-axis aligned along the beam line and the x-axis pointing towards the centre of the LHC ring. Pseudorapidity, η , is defined as

$$\eta = -\ln \tan \left(\frac{\theta}{2} \right) \quad (2.2)$$

where θ is the angle with respect to the z-axis.¹ Transverse energy, E_T , and transverse momentum, p_T , are also defined with respect to the z-axis as:

$$E_T = E \sin(\theta) \quad \text{and} \quad p_T = \vec{p} \sin(\theta) \quad (2.3)$$

¹Pseudorapidity is preferred to θ because differences in η are invariant under boosts along the z-axis. Pseudorapidity is equivalent to the more general quantity rapidity, $y = \frac{1}{2} \ln \left(\frac{E+p_z}{E-p_z} \right)$, when the mass of the particle can be neglected.

where E and \vec{p} are the energy and momentum of the relevant object. The azimuthal angle in the transverse plane, ϕ , is defined to be zero along the x-axis.

The detector itself is split into three sections. A cylindrical barrel surrounding the interaction point which provides coverage out to approximately $|\eta| < 1.4$ and two end-caps at either end of the barrel, covering $\sim 1.4 < |\eta| < 4.9$.

Each of the regions are split further into several sub-detectors. At the heart of ATLAS is the Inner Detector (ID) that enables measurements of the momentum of charged particles and accurate reconstruction of vertices produced by primary proton-proton collisions, as well as those that arise from the decay of long-lived particles. Surrounding the ID are the electromagnetic and hadronic calorimeters used to determine the energy of all charged and neutral particles. The outermost sub-detector is the Muon Spectrometer (MS), which enables precision measurements of the momentum of muons.

ATLAS contains both solenoidal (in the barrel) and toroidal (in barrel and end caps) magnet systems. The solenoid is aligned along the beam axis and provides a 2 T magnetic field. It completely surrounds the ID but has been designed to ensure that the material thickness in front of the calorimeters is as low as possible. Charged particles travelling through the solenoid have their trajectory curved in the ϕ -direction. The barrel and end-cap toroids produce 0.5 and 1 T magnetic fields, respectively. The toroid magnets enable measurements of the momentum of muons and cause the tracks produced by them to be curved in the η -direction. Measurements of the momentum of all charged particles are performed by measuring the curvature of the tracks produced by the particles as they traverse the detector subject to these magnetic fields.

2.2.1 The Inner Detector

The ATLAS Inner Detector (ID) is made up of three independent sub-detectors and in total is contained within a cylindrical region of length ± 3512 mm and radius 1150 mm. Closest to the beam is the pixel detector, followed by the semi-conductor tracker (SCT) and transition radiation tracker (TRT). The combination of the three complementary sub-detectors allows precision reconstruction of collision vertices, robust pattern recognition, and precision measurements of the momentum of charged particles produced with $|\eta| < 2.5$. It can also provide electron identification over $|\eta| < 2.0$ and a wide range of energies (0.5–150 GeV).

2.2.1.1 Pixel Sensors and Semi-conductor Trackers

Both the pixel and SCT sensors are made from silicon. A charged particle passing through the silicon creates electron-hole pairs and a potential difference applied across the silicon causes the charges to drift towards the readouts.

Each pixel module is $250\text{ }\mu\text{m}$ thick and allows double-sided processing. The module measures $19 \times 63\text{ mm}^2$ and contains $\sim 47,000$ pixels, each of which measures $50 \times 400\text{ }\mu\text{m}^2$. In total the pixel detector is made up of 1744 modules split between three barrel layers and two sets of three end-cap disks. The barrel layers have radii of 50.5, 88.5 and 122.5 mm and provide coverage out to $|\eta| < 1.7$ and complete azimuthal coverage. End-cap disks have $|z| = 495, 580$ and 650 mm and cover the range $1.7 < |\eta| < 2.5$. The spatial resolution of pixel modules varies with the incident angle of the particle from $12\text{ }\mu\text{m}$ at normal incidence, to an optimal resolution of $4.7\text{ }\mu\text{m}$ for incident angles of $10\text{--}15^\circ$.

The SCT sensors are made up of a series of single-sided p-in-n silicon microstrips of thickness $285 \pm 15\text{ }\mu\text{m}$. In the barrel, strips are created by joining two rectangular sensors with dimensions $6.39 \times 6.36\text{ cm}^2$. Each sensor has 768 strips with an $80\text{ }\mu\text{m}$ pitch, with four sensors making up one module, mounted back-to-back in pairs. There are 2112 modules in the barrel of the SCT, arranged in four layers and aligned such that the strips lie along the direction of the beam and offer precise measurements of the ϕ coordinate. The 1976 SCT modules making up the two end-caps are arranged in nine layers of disks. Each of the sensors in the end-caps are trapezoidal in shape and come in three sizes for separate construction of inner, middle and outer regions of the disk. The sensors are aligned with their microstrips in the radial direction, again allowing precise measurements of the ϕ coordinate. The spatial resolution of sensors in both the barrel and end-caps is $\sim 16\text{ }\mu\text{m}$ for normally-incident particles.

2.2.1.2 The Transition Radiation Tracker

The basic TRT detector elements are drift tubes (straws) of diameter 4 mm and length 144 cm (37 cm) in the barrel (end-caps). The straws are filled with a gas mixture of 70% Xe, 27% CO_2 and 3% O_2 . Charged particles passing through the straws cause ionisation of the gas, and the electrons that are produced drift towards a tungsten anode mounted at the centre of each tube. As in the pixel and SCT detectors, if the total charge collected is above some threshold it is defined as a particle hit. In the barrel the TRT contains ~ 52500 straws arranged in 73 layers and aligned in the z-direction, while each end-cap is made up of 160 planes of radially-aligned straws—over 120,000 straws per end-cap. Any charged particle with $p_T > 0.5\text{ GeV}$ will traverse at least 36 layers of straws, except in the transition region between the barrel and end-cap, where the number is reduced to a minimum of 22 crossed straws. Radiator material is placed between each of the straws. Highly relativistic particles crossing the boundary between radiator and straw emit transition radiation photons, which cause additional ionisation. Higher thresholds are defined to determine whether a hit contains transition radiation in addition to the particle itself.

2.2.2 The Calorimeters

ATLAS contains a number of calorimeters that measure the energy of incident particles through absorption. Alternating layers of absorber and sampling material cause particles entering the calorimeter to shower into secondary particles, the energy of which are collected and measured. The number of layers of material and the geometry of the calorimeter modules is such that the probability of particles ‘punching-through’ the calorimeters and escaping with some unmeasured energy is kept to a minimum.

2.2.2.1 Electromagnetic Calorimeters

The electromagnetic (EM) calorimeters use a combination of lead and liquid argon (LAr) layers to measure the energy of electrons and photons. On passing through the calorimeters electrons emit bremsstrahlung photons, which in turn can produce electron-positron pairs. The resulting shower of electromagnetic particles causes ionisation in the active LAr layers, with copper electrodes collecting the charge. An accordion-like geometry gives the barrel and end-cap EM calorimeters complete ϕ coverage without any cracks or gaps. In the barrel the EM calorimeter is made of two half-barrels. Each half-barrel is 3.2 m in length, weighs 57 tonnes and contains 1024 absorbers interleaved with readout electronics. Constructed in 16 separate modules, the barrel of the EM calorimeter provides between 22 and 33 radiation lengths (X_0) of material to try and keep punch-through of particles into the muon system to a minimum. In the region $|\eta| < 1.8$ a liquid-argon presampler layer is used to correct for energy lost by electrons or photons before reaching the calorimeter, such as through interactions with the ID or supporting structure.

The granularity of the barrel EM calorimeter varies between the three layers that make up each module. The second layer, consisting of 16 radiation lengths of material, absorbs the majority of the energy of the particles and has a granularity of 0.025×0.025 in $\eta \times \phi$. Such a fine granularity is ideally suited for precision measurements of electrons and photons.

The layout of the end-cap calorimeters is more complex. The two wheels, one at either end of the barrel, each weigh 27 tonnes and are made up of a series of wedge-shaped modules. The granularity and thickness of the wheels varies as a function of $|\eta|$. For $|\eta| > 1.475$ the thickness is greater than $24X_0$, and in the precision regions of the end-cap the granularity matches that of the barrel, $\eta \times \phi = 0.025 \times 0.025$.

2.2.2.2 Hadronic Calorimeters

The hadronic calorimeters are used to measure the energy of baryons and mesons. The tile calorimeter is constructed in three sections, a barrel and two extended barrels, providing coverage over the region $|\eta| < 1.7$. Each section is made up of 64 wedge-shaped modules, and each module uses layers of steel as the absorber material that

causes the particles to shower, and scintillating tiles as the active medium that sample the energy of the shower particles and produce detectable signals proportional to the energy. Each scintillating tile is coupled to a photomultiplier tube and readout electronics. Tiles are grouped to form cells with dimensions $\Delta\eta \times \Delta\phi = 0.1 \times 0.1$ in the first two layers and 0.2×0.1 in the last layer.

The hadronic end-cap (HEC) calorimeters cover the region $1.5 < |\eta| < 3.5$ and use copper sheets to provide the hadron shower and liquid-argon gaps for the active medium. As in the end-caps of the EM calorimeter, the granularity of the HEC varies with $|\eta|$, from $\Delta\eta \times \Delta\phi = 0.1 \times 0.1$ in the region $|\eta| < 2.5$, to 0.2×0.2 for larger values of η .

The forward calorimeters (FCal) extend the coverage of the calorimeters to $3.1 < |\eta| < 4.9$. Each FCal is made up of three modules: an electromagnetic module that uses copper as its main absorber material, and two hadronic modules which use tungsten. Liquid-argon is used as the active material in all three modules and they all make use of the same cryostat systems as the other end-cap calorimeters, reducing any gaps in coverage. At just 0.27 mm the liquid-argon gaps in the FCal are smaller than in the EM barrel calorimeter. This enables the FCal to provide faster signals, and deal with the large particle flux produced at low angles with respect to the beam.

2.2.3 The Muon Spectrometer

The ATLAS Muon Spectrometer (MS) has been designed to provide both triggering (See Sect. 2.2.4) and precision measurement capabilities. Both functions are performed in the barrel and end-caps, triggering on muons with $|\eta| < 2.4$ and precision tracking on muons with $|\eta| < 2.7$.

2.2.3.1 Precision Measurements

Precision measurements of muon momenta are performed by Monitored Drift Tubes (MDTs) in both the barrel and end-caps, apart from the innermost layer in the forward region $2 < |\eta| < 2.7$ where they are replaced by Cathode Strip Chambers (CSCs), for their higher rate capabilities.

Each MDT chamber is made up of two multi-layers (three or four layers, depending on the position of the chamber) of pressurised drift tubes. Muons traversing the chamber cause ionisation of the gas and the resultant electrons are collected by tungsten-rhenium wires held at the centre of each tube. The tubes have a diameter of 29.97 mm, are filled with a mixture of CO_2 and Ar and are aligned along ϕ in both the barrel and end-caps. In the barrel the MDT chambers are arranged in concentric layers around the beam axis and are mounted between and on the coils of the toroid magnets. In the two end-caps the MDTs form large wheels, and are located in front of and behind the two end-cap toroids. This configuration allows a precise measurement of the η -coordinate of the muons—the direction they are bent on passing through the

toroidal magnetic field. The resolution of a single MDT is $80\text{ }\mu\text{m}$, or about $35\text{ }\mu\text{m}$ per chamber.

The Cathode Strip Chambers are multi-wire proportional chambers with wires aligned in the radial direction. A single chamber is made of four planes of wires. Eight small and eight larger chambers make up one end-cap disk. Within each plane, one set of cathode strips is aligned parallel to the wires, while the other is oriented perpendicularly. This allows the CSCs to determine both the η and ϕ coordinates of the tracks at once, by reading out the charge induced on each set of cathode strips. The more precise measurement, in the bending direction, has a resolution of $60\text{ }\mu\text{m}$ while in the non-bending direction measurements are coarser with a resolution of around 5 mm .

2.2.3.2 Trigger Chambers

The trigger chambers comprise Resistive Plate Chambers (RPCs) in the barrel region $|\eta| < 1.05$ and Thin Gap Chambers (TGCs) in the end-cap $1.05 < |\eta| < 2.4$. Muon hit information is produced within a few tens of nanoseconds of the passage of the particle.

Contrary to the other technologies employed within the muon spectrometers, the RPCs contain no wires. Each is made up of two parallel resistive plates, with perpendicular sets of metallic strips mounted on the outer faces providing the signal readout, and gas filling the 2 mm gap in between. Charged particles passing through the RPCs ionise the gas, and a uniform 4.9 kV/mm electric field between the plates allows avalanches of electrons to form along the ionising tracks.

Most RPC chambers are made up of two rectangular detectors, or units, each of which consists of two independent gas volumes. The RPCs are arranged in three concentric cylinders around the beam axis, requiring in total 544 RPC chambers and 962 separate units. They are mounted above and below their MDT counterparts.

The TGCs are multi-wire proportional chambers with a gas gap of 2.8 mm filled with a mixture of CO_2 and $\text{n-C}_5\text{H}_{12}$ (n-pentane). They perform two main functions: triggering capabilities for muons with $1.05 < |\eta| < 2.4$ and measurements of the azimuthal coordinate of the muons, to complement the precise measurement of the coordinate in the bending direction performed by the MDTs. One chamber is made up of a gas volume, containing a wire plane, and two cathodes. Chambers are arranged in doublets or triplets to form each TGC unit. The cathode planes are coated on one side with graphite and on the other with copper. The copper layers are segmented into readout strips and are used to perform the measurement of the azimuthal coordinate.

2.2.4 Trigger and Data Acquisition

It is not possible to store the output of every proton-proton collision occurring within ATLAS. A single event recorded by ATLAS requires $\sim 1.5\text{ MB}$ of memory when

stored offline [11]. With a bunch cross frequency of 40 MHz at design luminosity, recording every event would therefore require data to be written to disk at a rate of $\sim 60 \text{ TBs}^{-1}$. The majority of these events do not contain objects such as hard jets or high- p_T leptons which are the signatures of many rarer, lower cross-section processes such as the production of top quarks or Higgs bosons. It would be preferable to only write such events to disk for detailed analysis.

The ATLAS trigger system identifies interesting events containing high- p_T objects in three distinct levels. The Level-1 (L1) trigger is hardware-based and reduces the event rate to 75 kHz. A decision to keep an event is made within $2.5 \mu\text{s}$. This is achieved through the use of reduced granularity information from a subset of the detectors. For example the RPC and TGC sections of the muon spectrometer are used to check whether muons with transverse momentum above specified thresholds are present in the event. All parts of the EM and hadronic calorimeters can be used to place requirements on the number and energy of electrons, photons, jets and τ -leptons, and also the amount of missing transverse energy, E_T^{miss} , and total transverse energy in each event.

If a physics object is found by the L1 trigger, its position is recorded and a region-of-interest (RoI) containing the object is passed on to the Level-2 (L2) trigger system. The L2 trigger reduces the event rate further to around 3.5 kHz, with the decision to keep the event made within 40 ms. The L2 algorithms use partial detector information from within the vicinity of the RoI to refine the objects reconstructed at L1.

The third and final level of the trigger system is the Event Filter (EF). The EF makes use of the full granularity of the detector to reduce the event rate to approximately 200 Hz. Algorithms similar to those used when reconstructing events offline are used to reconstruct the objects of interest.

Trigger nomenclature typically follows the format:

`Level_Stream&Cut_Note`. For example an event passing the trigger `L1_MU11` must contain a muon identified at L1 with $p_T > 11 \text{ GeV}$. `EF_mu24i_medium` requires events to contain an isolated muon with $p_T > 24 \text{ GeV}$ and the `medium` in this case refers to a specific L1 trigger that must also have fired.

Only once an event has passed an EF trigger is it written to disk for permanent storage. As data is being collected it is organised into *periods* and *runs*, which allows easy organisation and management of the huge amount of data collected by ATLAS. A run begins once the Data Acquisition (DAQ) infrastructure, detectors and other sub-systems are configured correctly, and once the conditions of the beam provided by the LHC are stable. A run is ended either cleanly when there is deemed to be sufficient data collected or is aborted when a problem occurs, for example if the LHC beams are lost. A period is defined as a succession of DAQ runs.

After data have been collected a series of further data quality checks are performed. If the data in the runs under scrutiny are of a sufficient quality, and all of the triggers and detector systems were functioning optimally, then the runs are added to a so-called *Good Runs List* (GRL). Only those runs which appear in a GRL can be used for physics analysis.

References

1. Evans, L., & Bryant, P. (2008). LHC Machine. In L. Evans (ed.), *JINST* 3 (S08001).
2. LEP Design Report. (1983). 1. The LEP injector chain.
3. LEP Design Report. (1984). Vol. 2. The LEP Main Ring.
4. Myers, S. (1991). The LEP collider, from design to approval and commissioning.
5. Chatrchyan, S., et al. (2008). The CMS experiment at the CERN LHC. *JINST*, 3, S08004.
6. Augusto Alves, A., et al. (2008). The LHCb Detector at the LHC. *JINST*, 3, S08005.
7. Aamodt, K., et al. (2008). The ALICE experiment at the CERN LHC. *JINST*, 3, S08002.
8. ATLAS Collaboration. (2013). Improved luminosity determination in pp collisions at $\sqrt{s} = 7$ TeV using the ATLAS detector at the LHC. *European Physical Journal C*, 73, 2518.
9. ATLAS Collaboration. (2014). Total integrated luminosity in 2011 and 2012. Retrieved March 12, 2014, from <https://twiki.cern.ch/twiki/bin/view/AtlasPublic/LuminosityPublicResults>.
10. ATLAS Collaboration. (2014). Number of interactions per crossing. Retrieved March 12, 2014, from <https://twiki.cern.ch/twiki/bin/view/AtlasPublic/LuminosityPublicResults>.
11. ATLAS Collaboration. (2014). ATLAS fact sheet. Retrieved April 8, 2014, from http://www.atlas.ch/pdf/ATLAS_fact_sheets.pdf.

QCD Radiation in Top-Antitop and Z+Jets Final States
Precision Measurements at ATLAS

Joshi, K.

2015, XVI, 178 p. 97 illus., 63 illus. in color., Hardcover

ISBN: 978-3-319-19652-7